

Supporting Information for

## Defect Engineering and Carbon Supporting to Achieve Ni Doped CoP<sub>3</sub> with High Catalytic Activities for Overall Water Splitting

Daowei Zha<sup>1,2</sup>, Ruoxing Wang<sup>1,2</sup>, Shijun Tian<sup>1</sup>, Zhong-Jie Jiang<sup>2,\*</sup>, Zejun Xu<sup>1</sup>, Chu Qin<sup>1</sup>, Xiaoning Tian<sup>3,\*</sup> and Zhongqing Jiang<sup>1,\*</sup>

<sup>1</sup> Department of Physics, Zhejiang Sci-Tech University, Hangzhou, 310018, P. R. China

<sup>2</sup> Guangzhou Key Laboratory for Surface Chemistry of Energy Materials, Guangdong Engineering and Technology Research Center for Surface Chemistry of Energy Materials, College of Environment and Energy, South China University of Technology, Guangzhou, 510006, P. R. China

<sup>3</sup> Department of Materials and Chemical Engineering, Ningbo University of Technology, Ningbo, 315211, P. R. China

\*Corresponding authors. E-mail: [eszjiang@scut.edu.cn](mailto:eszjiang@scut.edu.cn) or [zhongjiejiang1978@hotmail.com](mailto:zhongjiejiang1978@hotmail.com) (Zhong-Jie Jiang); [boxertxn@hotmail.com](mailto:boxertxn@hotmail.com) (Xiaoning Tian); [zhongqingjiang@zstu.edu.cn](mailto:zhongqingjiang@zstu.edu.cn) (Zhongqing Jiang)

### S1 Experimental Section

#### S1.1 Electrochemical Tests

All electrochemical tests were performed at room temperature on an electrochemical station (CHI 760E, CH Instruments Inc, Shanghai) in a standard three-electrode system. The prepared catalysts, a graphite electrode, and a saturated calomel electrode were used as the working, the counter, and the reference electrodes, respectively. 1.0 M KOH was used as the electrolyte. Before data collection, cyclic voltammetry (CV), scanned at 0.068-0.132 V vs. RHE at a scan rate of 50 mV s<sup>-1</sup>, was applied to electrochemically activate the catalysts.

Linear sweep voltammetry (LSV) was performed in 1.0 M KOH at 10 mV s<sup>-1</sup>. Tafel slopes were calculated based on the LSV curves. Electrochemical impedance spectra (EIS) were measured at an overpotential of 100 mV from 0.01 Hz to 100 KHz. All the measured potentials vs. the SCE were converted to vs. the RHE by the equation  $E_{RHE} = E_{SCE} + 0.059 \text{ pH} + 0.242$ . All the LSVs reported were iR collected.

ECSA was estimated based on the electrochemical double layer capacitance  $C_{dl}$ , determined from the CVs measured at different scan rates in the non-Faraday potential region. In this work, since carbon cloth was used as the substrate, which has a certain capacitance value (as shown in Fig. S8), the capacitance of carbon cloth was used as the standard value, and the ECSA of each catalyst was calculated by the following formula:

$$ECSA = \frac{C_{dl} \text{ of catalyst (mF cm}^{-2}\text{)}}{C_{dl} \text{ of carbon cloth (mF cm}^{-2}\text{) per ECSA cm}^2} \quad (S1)$$

Taking the p-NiCoP/NCFs@CC as an example, in the HER, its ECSA could be calculated as:

$$ECSA_{p\text{-NiCoP/NCFs@CC}} = \frac{277 \text{ mF cm}^{-2}}{9 \text{ mF cm}^{-2} \text{ per cm}^2_{ECSA}} = 30.78 \text{ cm}^2_{ECSA} \quad (S2)$$

The TOF values were calculated according to previous reports [S1, S2]:

$$TOF = j \times \frac{A}{n \times F \times m} \text{ S}^{-1} \quad (S3)$$

where,  $j$  is the current density ( $A\ cm^{-2}$ ).  $A$  is the area of the carbon cloth electrode ( $cm^2$ ).  $n$  is the number of electrons transferred (for OER  $n = 4$  and for HER  $n = 2$ ).  $F$  is the Faraday constant (a value of  $96485\ C\ mol^{-1}$ ).  $m$  is the number of moles of the effective surface sites that are grown onto the carbon cloth.

The total number of effective surface sites was calculated based on the following equation:

$$\frac{\# \text{ Surface sites}}{cm^2 \text{ geometric area}} = \frac{\# \text{ Surface sites (flat standard)}}{cm^2 \text{ geometric area}} \times \text{Roughness factor} \quad (S4)$$

here the roughness factor ( $R_f$ ) can be determined by the  $C_{dl}$  from **Fig. S8**, and we assume  $60\ \mu F\ cm^{-2}$  for a flat electrode provided by previous reports [S3]. The surface sites of  $2 \times 10^{15}$  for the flat standard electrode was used for our calculation according to previous results. Thus, using the formula above, the number of surface active sites for the p-NiCoP/NCFs@CC catalyst is estimated to be  $2.15 \times 10^{18}$  surface sites  $cm^{-2}$ . Therefore, the TOF for the p-NiCoP/NCFs@CC catalyst at different overpotentials ( $\eta$ ) is calculated.

The amounts of the generated  $H_2$  and  $O_2$  were measured by a drainage method. Specifically, the generated  $H_2$  and  $O_2$  during the water splitting were separately flowed into the drain bottles filled with water. The amounts of the generated  $H_2$  and  $O_2$  can be directly obtained by measuring the volumes of the drained water.

The Faraday efficiency calculation formula:

$$\text{The Faraday efficiency} = \frac{\text{actual hydrogen or oxygen production}}{\text{current} * \text{time} * 0.01119} * 100\% \quad (S5)$$

## S1.2 DFT Calculation

The dipole corrected DFT calculations with considerations of spin polarization were performed in use of the Vienna ab-initio simulation package (VASP) [S4]. The electron–electron exchange correlations were described by the generalized gradient approximation (GGA) in the form of the Perdew-Burke-Ernzerhof (PBE) [S5]. The electron-ion interactions were described using the projector augment wave (PAW) type pseudopotential [S6]. An energy cut-off of  $450\ eV$  was employed for plane-wave expansion. The respective convergence criteria for energy and force were  $1 \times 10^{-5}\ eV$  and  $0.02\ eV\ \text{\AA}^{-1}$ . The Brillouin zone was sampled with the  $\Gamma$ -centered  $k$ -point mesh for the cell and slab optimization, which was selected to ensure  $a_n \times k_n$  ( $n = 1, 2, 3$ )  $> 30\ \text{\AA}$  ( $a_n$  is the lattice parameters of a cell). Calculations of the HER/OER energetics were carried out on the (200) surface of the cubic structure of  $CoP_3$  with some Co atoms replaced by Ni (NiCoP(200)). The NiCoP(200) with  $P_v$  (NiCoP(200)<sub>def</sub>) is achieved by removal of the P atoms from the NiCoP(200). To construct the model of the NiCoP(200)<sub>def</sub>/Gr, a NiCoP(200)<sub>def</sub> slab is stacked on the graphene substrate directly. The NiCoP(200)<sub>def</sub>-NiCoO/Gr slab was established by adding a layer of Ni doped  $Co_3O_4$  on the surface of the NiCoP(200)<sub>def</sub>/Gr. A vacuum slab of  $> 15\ \text{\AA}$  in  $z$ -direction was added to avoid the artificial interactions between the periodic images. The hydrogen adsorption free energy was computed using the equation:

$$\Delta G_{H^*} = (E_{\text{surface+H}} - E_{\text{surface}}) - 1/2E_{H_2} + \Delta ZPE - T\Delta S \quad (S6)$$

Where  $\Delta ZPE$  and  $\Delta S$  are the difference in the zero-point energy and entropy between the adsorbed H atom and the gaseous phase  $H_2$ . The OER activities of the catalyst were evaluated based on the models developed by Nørskov et al.[S7] It involves our elementary steps. The Gibbs free energy change ( $\Delta G$ ) of each step were computed by the following equation:

$$\Delta G = \Delta E + \Delta ZPE - T\Delta S + \Delta G_U + \Delta G_{pH} \quad (S7)$$

Where  $\Delta E$  is the binding energy change of the intermediates,  $\Delta ZPE$  and  $\Delta S$  are the zero-point and entropy changes of each step.  $\Delta G_U = -eU$  ( $U$  is the applied potential).  $\Delta G_{pH}$  is the pH value correlation of  $\Delta G$ :  $\Delta G_{pH} = k_B T \ln(10) \times pH$ .

## S2 Supplementary Figures and Tables

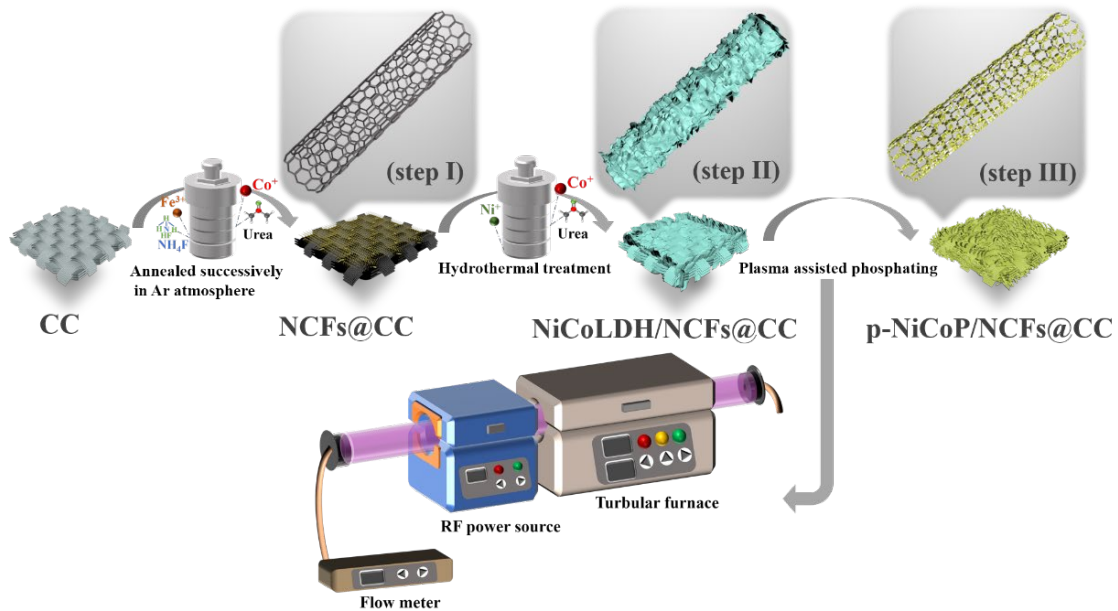


**Fig. S1** Illustration of the procedure for the synthesis of the p-NiCoP/NCFs@CC

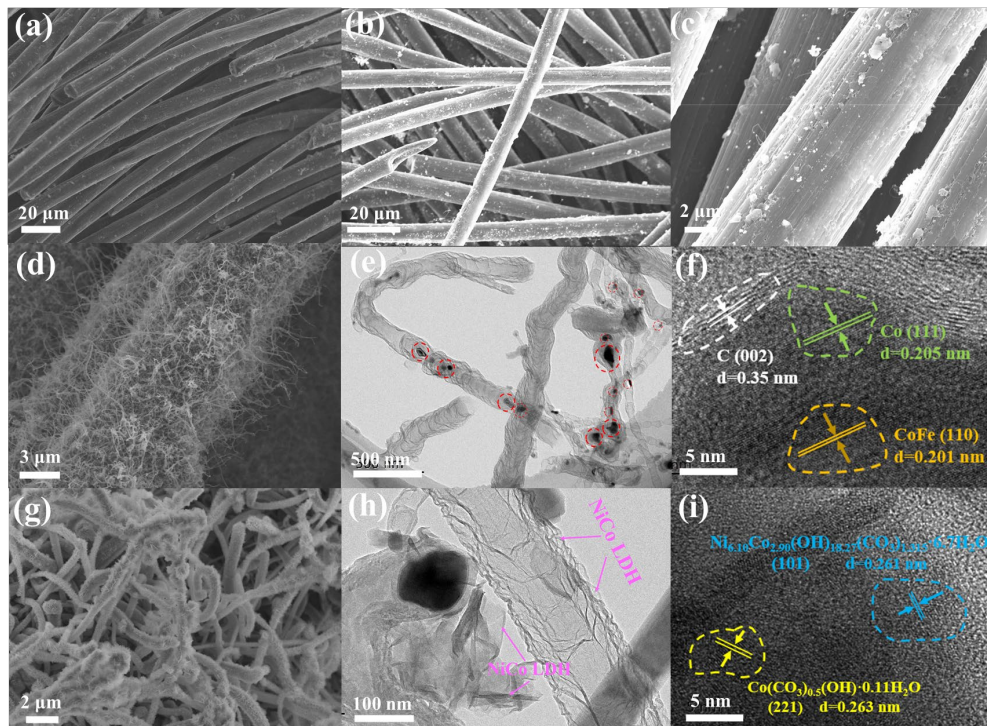


**Fig. S2** a SEM image of CC, b, c SEM images of the CC calcined in the presence of dicyandiamide without the FeCo LDH deposition, d SEM image of NCFs@CC, e TEM and f HRTEM images of NCFs scraped from the NCFs@CC, g SEM image of NiCoLDH/NCFs@CC, h TEM and i HRTEM images of NiCoLDH scraped from the NiCoLDH/NCFs@CC

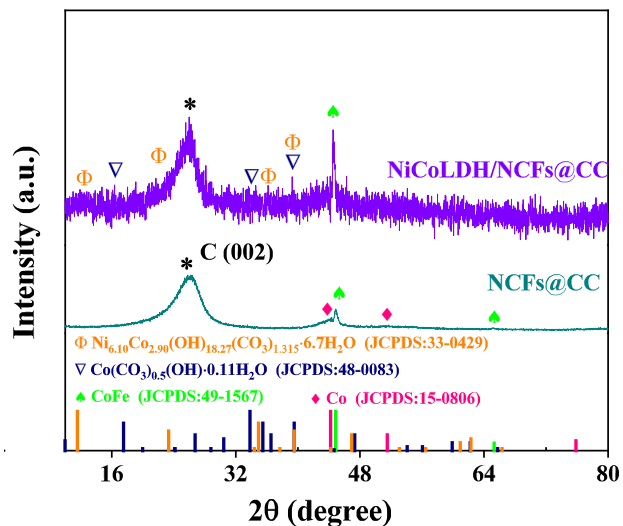


Fig. S3 XRD patterns of NCFs@CC and NiCoLDH@NCFs@CC

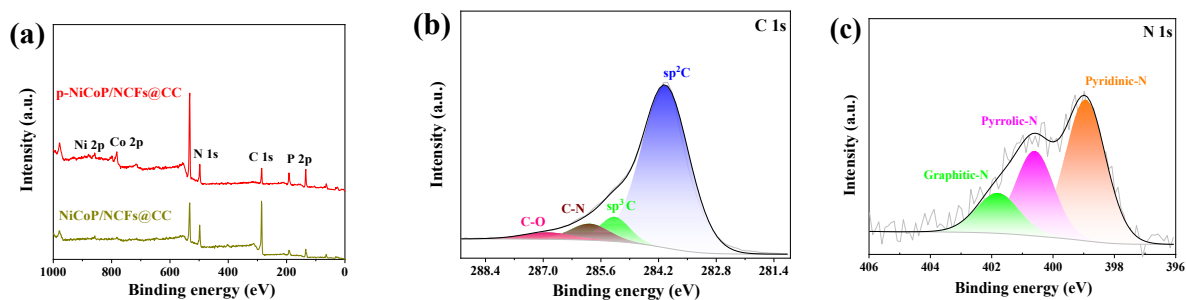


Fig. S4 a XPS survey spectrum of p-NiCoP/NCFs@CC. b C 1s and c N 1s spectra of p-NiCoP/NCFs@CC

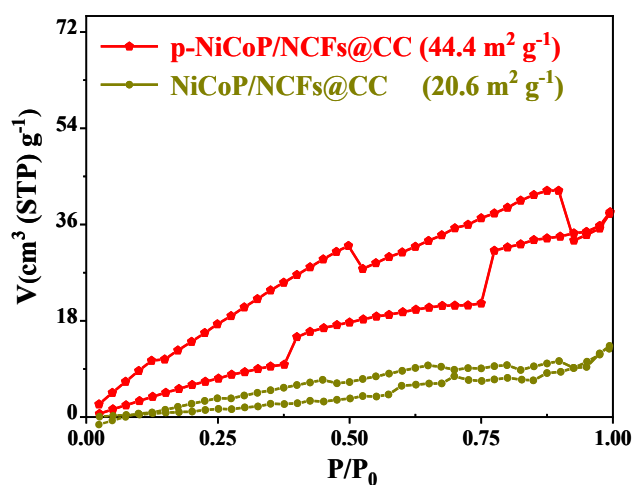
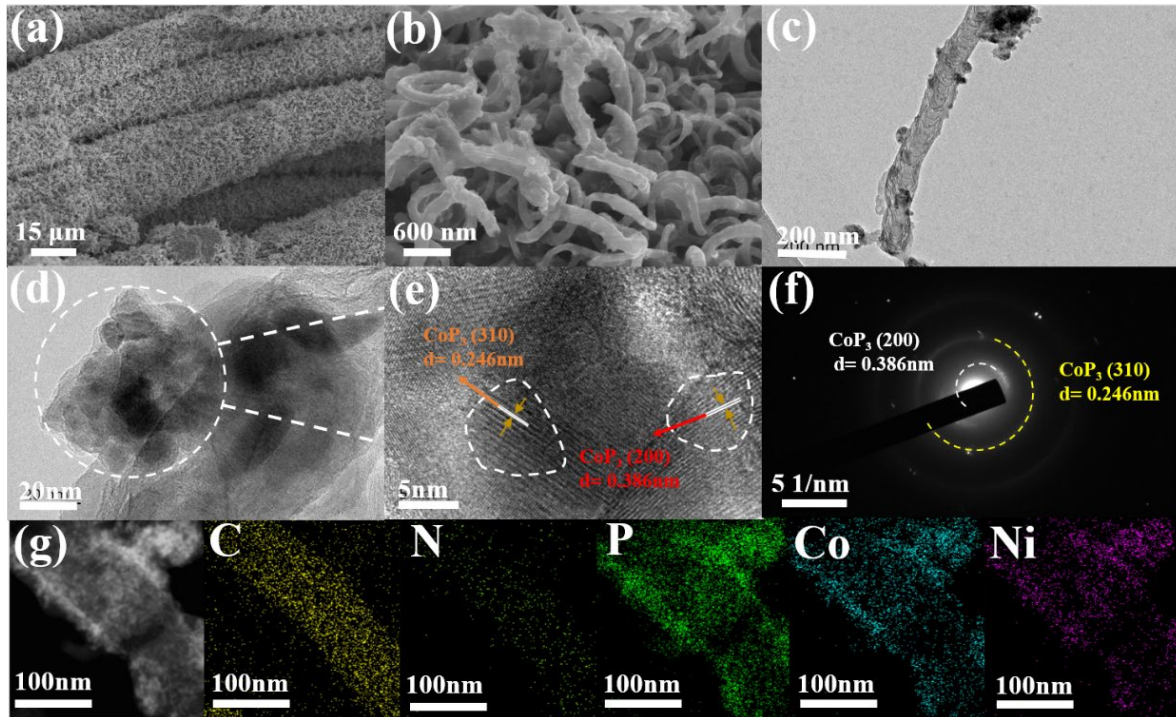
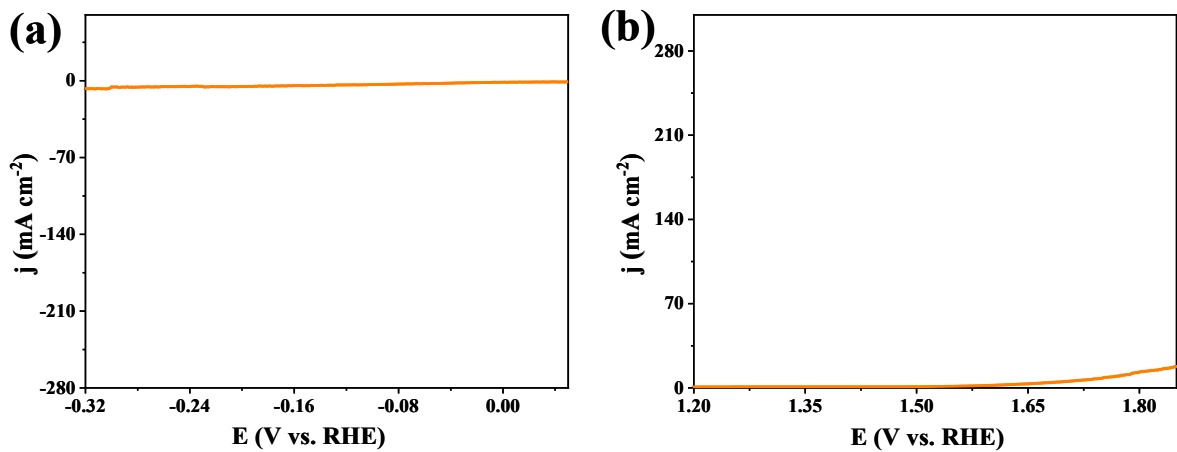


Fig. S5 N<sub>2</sub> adsorption-desorption isotherms



**Fig. S6** **a, b** SEM images of NiCoP/NCFs@CC, **c, d** TEM, **e** HRTEM, **f** SAED pattern, and **g** EDX elemental mapping images of NiCoP/NCFs scraped from the NiCoP/NCFs@CC



**Fig. S7** **a** HER and **b** OER polarization curves of the CC

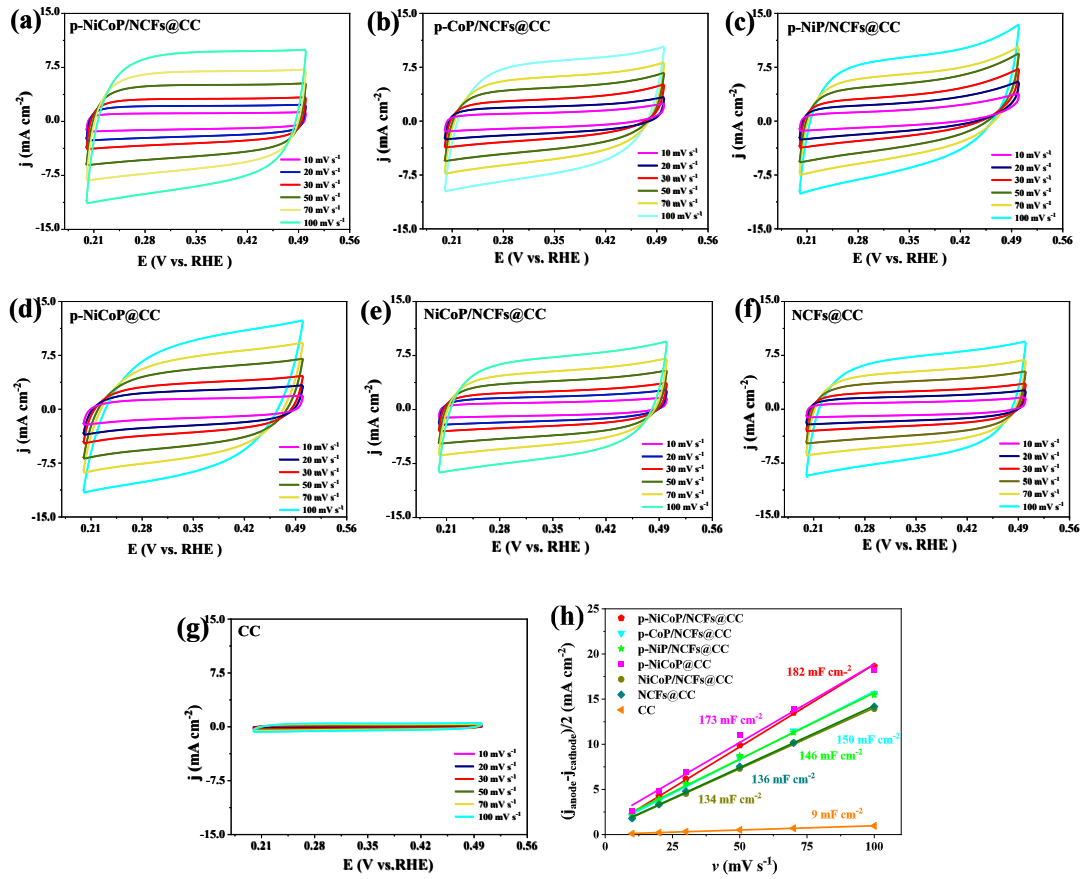


**Fig. S8** a-g Electrochemical CVs of the samples at different scanning rates ( $v$ ), **h** plot of  $(j_{\text{anode}} - j_{\text{cathode}})/2$  vs. scan rate ( $v$ ), whose slope corresponds to  $C_{dl}$  of the catalyst

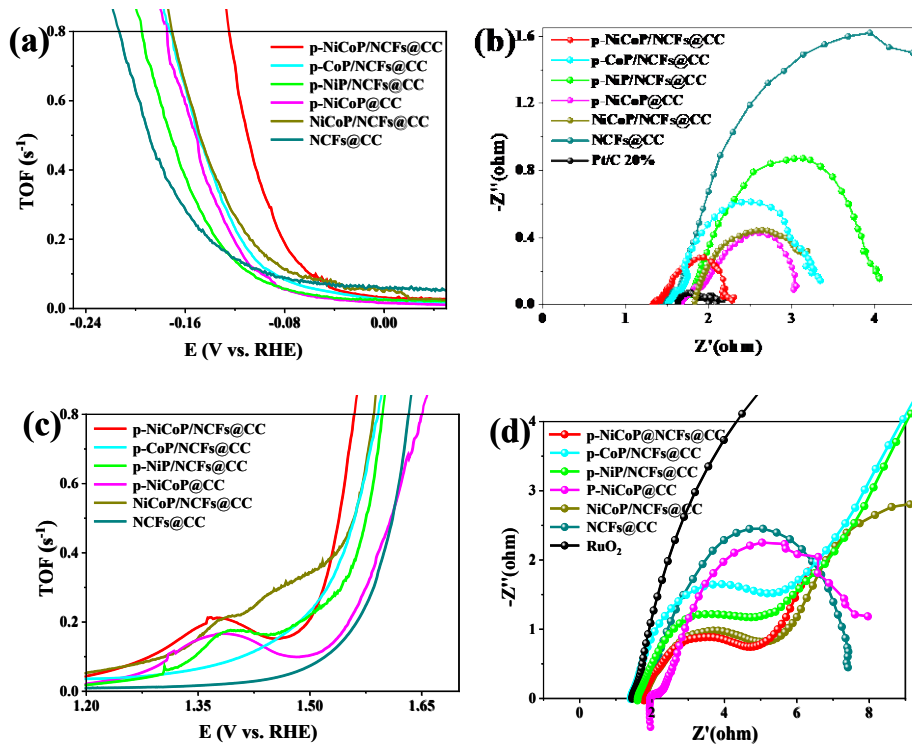


**Fig. S9** TOFs of the catalysts for **a** the HER and **c** the OER. EIS spectra of the catalysts for **b** the HER and **d** the OER

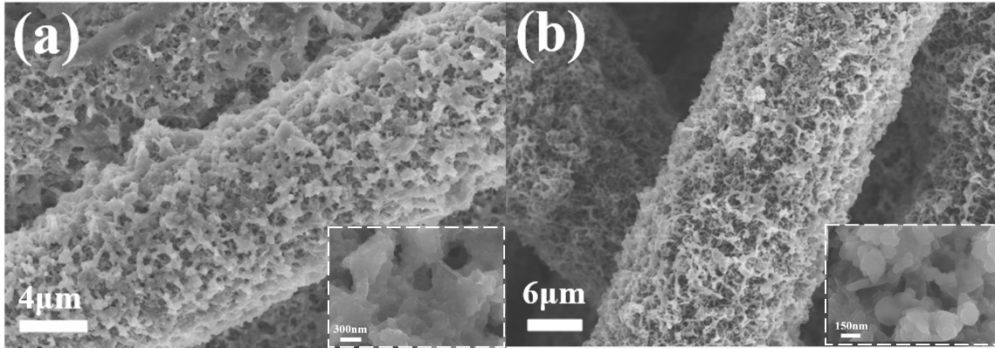


Fig. S10 SEM images of p-NiCoP/NCFs@CC after **a** the HER and **b** the OER.

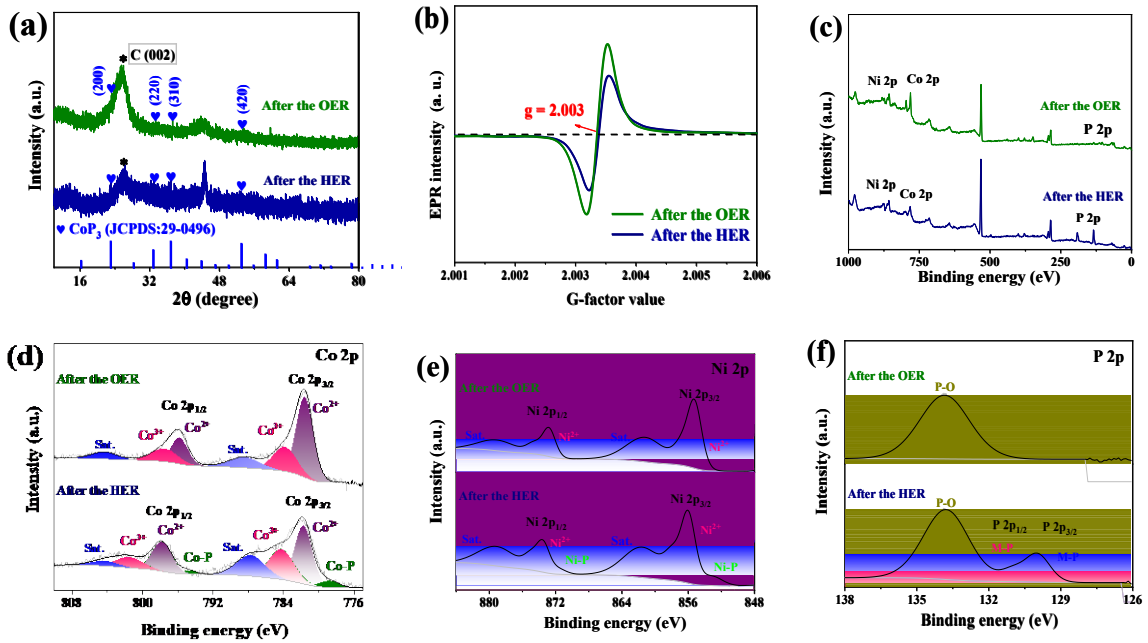


Fig. S11 **a** XRD pattern, **b** EPR spectra, and **c** XPS survey spectra of the p-NiCoP/NCFs@CC after the HER and the OER. XPS spectra of **d** Co 2p, **e** Ni 2p and **f** P 2p of the p-NiCoP/NCFs@CC after the HER and the OER

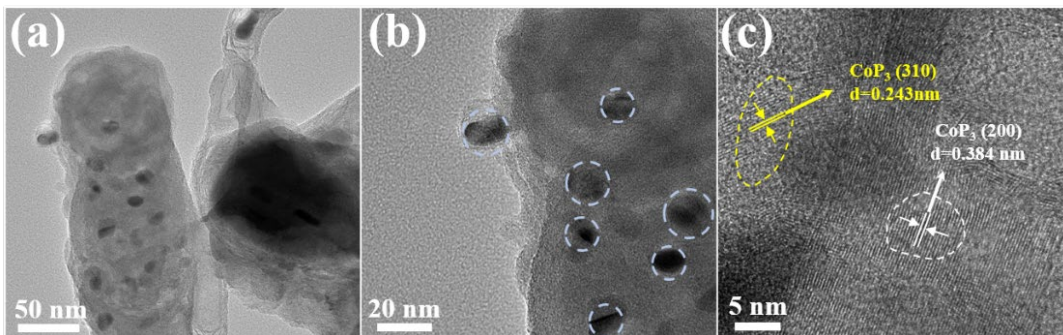
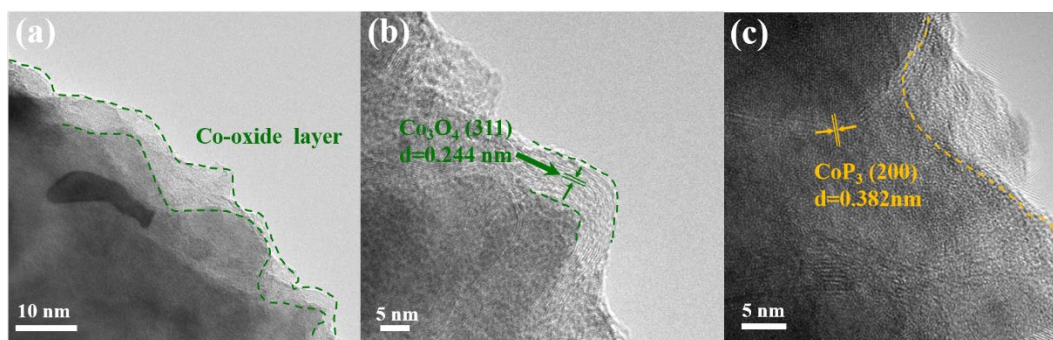
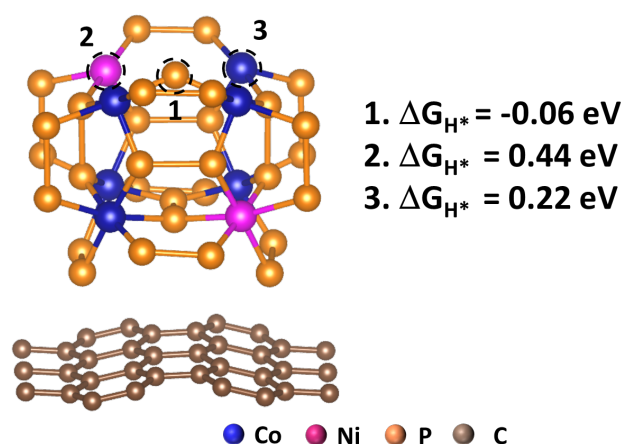


Fig. S12 **a** TEM, **b**, **c** HRTEM images of p-NiCoP/NCFs@CC scraped from the p-NiCoP/NCFs@CC after the HER



**Fig. S13** a TEM and b, c HRTEM images of p-NiCoP/NCFs@CC after the OER



**Fig. S14**  $\Delta G_{H^*}$  values of the H adsorption at the different sites on the NiCoP(200)<sub>def</sub>/Gr. It indicates that the P atom close to the Pv is the active site for the HER since it has a  $\Delta G_{H^*}$  value of -0.06 eV

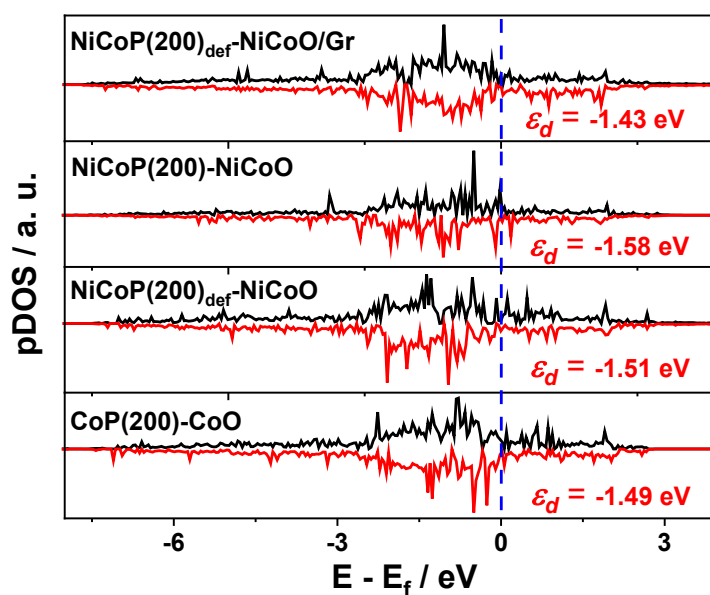


**Fig. S15** PDOSs of Co 3d for the NiCoP(200)<sub>def</sub>-NiCoO/Gr, the NiCoP(200)-NiCoO, the NiCoP(200)<sub>def</sub>-NiCoO, and the CoP(200)-CoO. The d-band centers of Co 3d are indicated

**Table S1** HER performance comparison of p-NiCoP/NCFs@CC with other TMPs based electrocatalysts

Catalyst	Electrolyte	$\eta$ (mV)	Tafel slope (mV dec <sup>-1</sup> )	Refs.
<b>p-NiCoP/NCFs@CC</b>	<b>1.0 M KOH</b>	<b><math>\eta_{10} = 29</math> <math>\eta_{50} = 86</math></b>	<b>68</b>	<b>This work</b>
NMCP@NF	1.0 M KOH	$\eta_{50} = 143$	70	[S8]
MnCoP/CC	1.0 M KOH	$\eta_{10} = 69$	46.16	[S9]
CeO <sub>2</sub> -NiCoP <sub>x</sub> /NCF	1.0 M KOH	$\eta_{10} = 39$	67	[S10]
FN-CoP NS	1.0 M KOH	$\eta_{10} = 66$	44.9	[S11]
NiFeCuP	1.0 M KOH	$\eta_{10} = 86$	52.3	[S12]
CoFeP NS@NCNF	1.0 M KOH	$\eta_{10} = 113$	108	[S13]
NiCoO-2P/S	1.0 M KOH	$\eta_{10} = 143$	82	[S14]
Cu <sub>3</sub> P/Ni <sub>2</sub> P@CF	1.0 M KOH	$\eta_{10} = 88.1$	94	[S15]
MoP@N-NiCoP	1.0 M KOH	$\eta_{10} = 43$	52	[S16]

**Table S2** OER performance comparison of p-NiCoP/NCFs@CC with other TMPs based electrocatalysts

Catalyst	Electrolyte	$\eta$ (mV)	Tafel slope (mV dec <sup>-1</sup> )	Refs.
<b>p-NiCoP/NCFs@CC</b>	<b>1.0 M KOH</b>	<b><math>\eta_{50} = 276</math> <math>\eta_{100} = 306</math></b>	<b>97</b>	<b>This work</b>
NMCP@NF	1.0 M KOH	$\eta_{50} = 280$	41	[S8]
MnCoP/CC	1.0 M KOH	$\eta_{100} = 460$	44.9	[S9]
CeO <sub>2</sub> -NiCoP <sub>x</sub> /NCF	1.0 M KOH	$\eta_{10} = 260$	72	[S10]
FN-CoP NS	1.0 M KOH	$\eta_{10} = 241$	69.6	[S11]
NiFeCuP	1.0 M KOH	$\eta_{10} = 156$	21.4	[S12]
CoFeP NS@NCNF	1.0 M KOH	$\eta_{20} = 268$	116	[S13]
NiCoO-2P/S	1.0 M KOH	$\eta_{100} = 254$	88	[S14]
Cu <sub>3</sub> P/Ni <sub>2</sub> P@CF	1.0 M KOH	$\eta_{50} = 330$	72	[S15]
MoP@N-NiCoP	1.0 M KOH	$\eta_{10} = 232$	45.85	[S16]

**Table S3** Cell performance comparison of the p-NiCoP/NCFs@CC with other water electrolyzers for overall water splitting

Catalyst	Electrolyte	Cell voltage(V) @10 mA cm <sup>-2</sup>	Refs.
p-NiCoP/NCFs@CC	1.0 M KOH	1.325	This work
NMCP@NF	1.0 M KOH	1.52	[S8]
MnCoP/CC	1.0 M KOH	1.68	[S9]
CeO <sub>2</sub> -NiCoP <sub>x</sub> /NCF	1.0 M KOH	1.49	[S10]
FN-CoP NS	1.0 M KOH	1.57	[S11]
NiFeCuP	1.0 M KOH	1.49	[S12]
CoFeP NS@NCNF	1.0 M KOH	1.59	[S13]
NiCoO-2P/S	1.0 M KOH	1.50	[S14]
Cu <sub>3</sub> P/Ni <sub>2</sub> P@CF	1.0 M KOH	1.56	[S15]
MoP@N-NiCoP	1.0 M KOH	1.54	[S16]

### Supplementary References

- [S1] J. Jia, L. Li, X. Lian, M. Wu, F. Zheng et al., A mild reduction of Co-doped MnO<sub>2</sub> to create abundant oxygen vacancies and active sites for enhanced oxygen evolution reaction. *Nanoscale* **13**, 11120-11127 (2021). <http://doi.org/10.1039/D1NR02324A>
- [S2] M. Duraivel, S. Nagappan, K.H. Park, K. Prabakar, Hierarchical 3D flower like cobalt hydroxide as an efficient bifunctional electrocatalyst for water splitting. *Electrochim. Acta* **411**, 140071 (2022). <https://doi.org/10.1016/j.electacta.2022.140071>
- [S3] H. Zhou, F. Yu, Y. Huang, J. Sun, Z. Zhu et al., Efficient hydrogen evolution by ternary molybdenum sulfoselenide particles on self-standing porous nickel diselenide foam. *Nat. Commun.* **7**, 12765 (2016). <http://doi.org/10.1038/ncomms12765>
- [S4] G. Kresse, J. Furthmüller, Efficient iterative schemes for ab initio total-energy calculations using a plane-wave basis set. *Phys. Rev. B* **54**, 11169-11186 (1996). <http://doi.org/10.1103/PhysRevB.54.11169>
- [S5] J.P. Perdew, K. Burke, M. Ernzerhof, Generalized gradient approximation made simple. *Phys. Rev. Lett.* **77**, 3865-3868 (1996). <http://doi.org/10.1103/PhysRevLett.77.3865>
- [S6] S. Goedecker, M. Teter, J. Hutter, Separable dual-space Gaussian pseudopotentials. *Phys. Rev. B* **54**, 1703 (1996). <https://doi.org/10.1103/PhysRevB.54.1703>
- [S7] J.K. Nørskov, J. Rossmeisl, A. Logadottir, L. Lindqvist, J.R. Kitchin et al., Origin of the overpotential for oxygen reduction at a fuel-cell cathode. *J. Phys. Chem. B* **108**, 17886-17892 (2004). <https://doi.org/10.1021/jp047349j>
- [S8] M.R. Kandel, U.N. Pan, D.R. Paudel, P.P. Dhakal, N.H. Kim et al., Hybridized bimetallic phosphides of Ni-Mo, Co-Mo, and Co-Ni in a single ultrathin-3D-nanosheets for efficient HER and OER in alkaline media. *Compos. Part B-Eng.* **239**, 109992 (2022). <https://doi.org/10.1016/j.compositesb.2022.109992>

- [S9] M. Wang, W. Fu, L. Du, Y. Wei, P. Rao et al., Surface engineering by doping manganese into cobalt phosphide towards highly efficient bifunctional HER and OER electrocatalysis. *Appl. Surf. Sci.* **515**, 146059 (2020). <https://doi.org/10.1016/j.apsusc.2020.146059>
- [S10] S. Wen, J. Huang, T. Li, W. Chen, G. Chen et al., Multiphase nanosheet-nanowire cerium oxide and nickel-cobalt phosphide for highly-efficient electrocatalytic overall water splitting. *Appl. Catal. B: Environ.* **316**, 121678 (2022). <https://doi.org/10.1016/j.apcatb.2022.121678>
- [S11] D. Xu, J. Yao, X. Ma, Y. Xiao, C. Zhang et al., F, N neutralizing effect induced Co-P-O cleaving endows CoP nanosheets with superior HER and OER performances. *J. Colloid Interf. Sci.* **619**, 298-306 (2022). <https://doi.org/10.1016/j.jcis.2022.03.123>
- [S12] J. Ge, S. Diao, J. Jin, Y. Wang, X. Zhao et al., NiFeCu phosphides with surface reconstruction via the topotactic transformation of layered double hydroxides for overall water splitting. *Inorg. Chem. Front.* **10**, 3515-3524 (2023). <http://doi.org/10.1039/D2QI02582E>
- [S13] B. Wei, G. Xu, J. Hei, L. Zhang, T. Huang et al., CoFeP hierarchical nanoarrays supported on nitrogen-doped carbon nanofiber as efficient electrocatalyst for water splitting. *J. Colloid Interf. Sci.* **602**, 619-626 (2021). <https://doi.org/10.1016/j.jcis.2021.06.045>
- [S14] F. Yan, L. Yan, X. Wei, Y. Han, H. Huang et al., Structure-design and synthesis of nickel-cobalt oxide/sulfide/phosphide composite nanowire arrays for efficient overall water splitting. *Int. J. Hydrogen Energy* **47**, 10616-10627 (2022). <https://doi.org/10.1016/j.ijhydene.2022.01.108>
- [S15] H. Liu, J. Gao, X. Xu, Q. Jia, L. Yang et al., Oriented construction Cu<sub>3</sub>P and Ni<sub>2</sub>P heterojunction to boost overall water splitting. *Chem. Eng. J.* **448**, 137706 (2022). <https://doi.org/10.1016/j.cej.2022.137706>
- [S16] Y. Zhang, X. Song, X. Guo, X. Li, Design of molybdenum phosphide @ nitrogen-doped nickel-cobalt phosphide heterostructures for boosting electrocatalytic overall water splitting. *J. Colloid Interf. Sci.* **648**, 585-594 (2023). <https://doi.org/10.1016/j.jcis.2023.05.202>